CRYSTAL GROWTH & DESIGN

Article

pubs.acs.org/crystal

Effects of Donor and Acceptor Units Attached with Benzoselenadiazole: Optoelectronic and Self-Assembling Patterns

Sahidul Mondal,[†] Maruthi Konda,[†] Brice Kauffmann,[‡] Manoj K. Manna,[†] and Apurba K. Das*[,†]

[†]Department of Chemistry, Indian Institute of Technology Indore, Indore 452017, India

[‡]CNRS UMS3033, INSERM US001, Institut Européen de Chimie et Biologie (IECB), Université de Bordeaux, , 2 rue Escarpit, 33600 Pessac, France

Supporting Information

ABSTRACT: Here, we report the effects of electron donor and acceptor units attached with benzoselenadiazole for the change in optoelectronic and packing patterns in solid states. We have synthesized 4-methoxybenzene, naphthalene, and 4-nitrobenzene capped benzoselenadiazoles (compounds **1**−**3** respectively) and studied their photophysical as well as electrochemical properties. All three molecules show two absorption bands (π−π transition band and CT-band). Three molecules (**1**−**3**) show orange, yellow-green, and green colors in dichloromethane solutions upon irradiation of UV light at 365 nm. Benzoselenadiazole-based compounds **1**−**2** form head to head dimers via Se···N interactions in the solid states. Compounds **1** and **2** show interlock type packing via Se···N interaction in their solid state structures. Se···π interaction takes a major role to form interlocked sheet type structures in crystal packing of compound **1**, whereas Se···N, N···N, and CH···π interactions help to form a supramolecular sheet type of structure in the crystal packing of compound **2**. Band gaps of these compounds were tuned by changing the electron donating to electron withdrawing units attached with a benzoselenadiazole core.

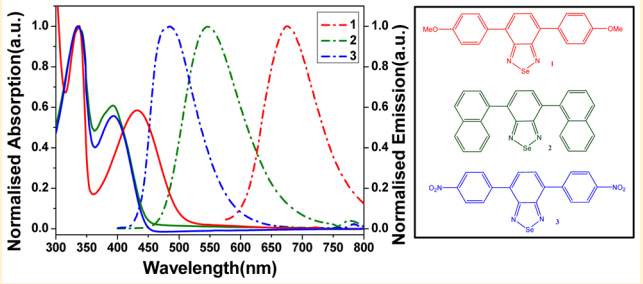

A wide range of π-conjugated systems are investigated for exploitation in device applications. Aromatic π-conjugated optoelectronic materials are important because they provide optical, electronic, and optoelectronic behavior. Aromatic π-conjugated molecules serve as active materials for the development of devices, in particular, for field-effect transistors, light-emitting diodes, and photovoltaics.[1−3] Small π-conjugated donor−acceptor−donor (D-A-D) systems as optoelectronic materials have been well developed. The optical and electronic properties of small conjugated molecules can be tuned by a small change in their molecular architectures.[4−6] π-Conjugated DAD systems are also used in conjugated polymers for the development of field effect transistors and solar cells. Donor−acceptor (D-A) based conjugated compounds have a low band gap and wide light absorption spectra.[7] Especially for the D−A systems, intramolecular charge transfer occurs from the electron-rich donor to electron-deficient acceptor units. Benzooxadiazole (BDO),[8−11] benzothiadiazole (BDT),[12−15] and benzoselenadiazole (BDS)[16−18] based acceptor units were used in conjugated molecules for the development of several electronic devices. Nevertheless, benzoselenadiazole-based molecules have also been used as probes for enzymes[19] and anions sensing.[20]

Wong et al. reported benzochalocogenodiazole-based D-A-A configured molecular donors for the development of organic solar cells.[21] Structural and optoelectronic properties of benzoselenadiazole containing DAD-based small molecules were described by Zade et al. to understand the substitution pattern of donor aromatic units attached with acceptor benzoselenadiazole unit.[22] Mikroyannidis et al. investigated the incorporation of low band gap Se-based small organic molecules in copolymer solar cells which show improved photovoltaic properties due to the increase in crystalline nature.[23] Recently, Patil et al. investigated in detail the change in electrical and optical properties by comparing two DAD molecules differing only by a chalcogen atom.[24] The band gap of D-A systems can be tuned by replacing with a heteroatom in an acceptor unit as well as by changing the donor unit. However, the number of reported examples with A-A units is very limited.

In this paper, we report synthesis, optical, packing patterns, electrochemical, and theoretical studies of BDS containing molecules **1**, **2**, and **3** (Scheme 1). To study the effect of donor and acceptor units attached with BDS, we have synthesized 4-methoxybenzene (compound **1**), naphthalene (compound **2**), and 4-nitro benzene (compound **3**) capped benzoselenadiazoles. The optical properties of compounds **1**−**3** were studied in an organic solvent dichloromethane. Compounds **1** and **2** show strong Se···N interaction, which facilitates the formation of a head to head pairwise dimer structure. In higher order self-

Received: August 17, 2015
Revised: September 27, 2015

DOI: 10.1021/acs.cgd.5b01179
Cryst. Growth Des. XXXX, XXX, XXX−XXX

Scheme 1. Synthesis of Compounds 1, 2, and 3[a]

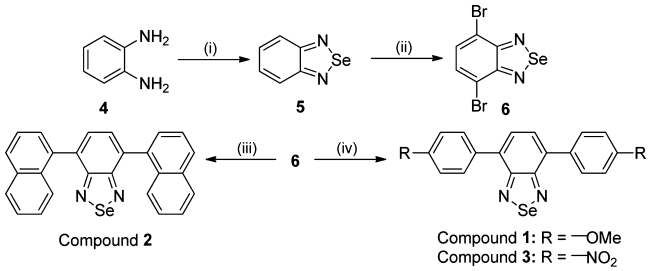

[a]Reagents and conditions: (i) SeO_2, EtOH, 1 h reflux; (ii) Ag_2SO_4, H_2SO_4, Br_2; (iii) naphthaleneboronic acid, K_2CO_3, $Pd(PPh_3)_4$, THF/water, 85 °C, 12 h, yield = 72% (compound **2**); (iv) *para* substituted benzeneboronic acid, K_2CO_3, $Pd(PPh_3)_4$,THF/water, 80 °C,12 h, yield = 81% (compound **1**), 66% (compound **3**).

assembly, compounds **1** and **2** stack to form an interlocked structure using hydrogen bonding, C—H···π and π—π stacking interactions. Compounds **1** and **2** showed strong orange and yellow-green emissions in dichloromethane solution respectively, whereas compound **3** shows green emission due to the presence of a strong electron withdrawing 4-nitrobenzene group with a central BDS unit (Figure 1).

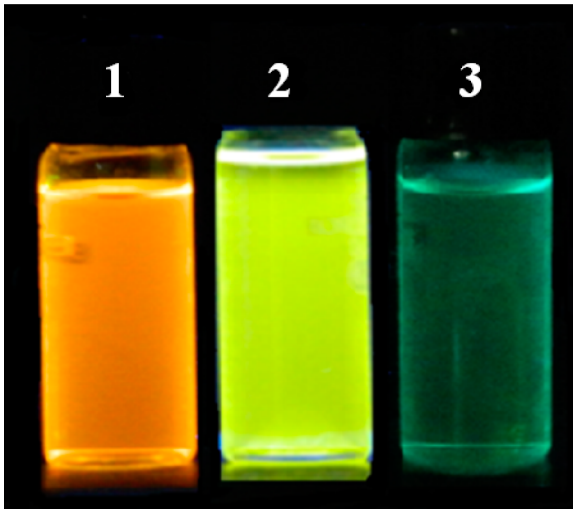

Figure 1. Photographs of compounds **1**, **2**, and **3** in dichloromethane solutions under a 365 nm UV lamp.

EXPERIMENTAL SECTION

General Methods. All reagents and chemicals were obtained commercially. All the reactions were performed under nitrogen atmosphere using a standard method. Toluene and tetrahydrofuran (THF) were distilled from sodium/benzophenone prior to use. Dichloromethane and hexane were also distilled from calcium chloride for purification purposes. DCM was freshly distilled from CaH_2 prior to use for optical and electrochemical studies. Final compounds were purified by using silica gel column (60—120 mesh). The hexane/DCM (9:1) system for compound **2** and the toluene/ethyl acetate (9:1) system for compounds **1** and **3** were used for purification purposes. ^{1}H NMR (400 MHz) and ^{13}C NMR (100 MHz) spectra were recorded on a Bruker AV 400 MHz spectrometer at 300 K. Compound concentrations were in the range 5—10 mmol L^{-1} in $CDCl_3$. UV—vis absorption spectra of all compounds were recorded using a Varian Cary100 Bio UV—vis spectrophotometer. Fluorescence spectra of all compounds were recorded on Horiba Scientific Fluoromax-4 spectrophotometer (Horiba Jobin Yvon) with a 1 cm path length quartz cell at room temperature. HRMS spectra were recorded on a Bruker micrOTOF-Q II mass spectrometer. The density functional theory (DFT) calculations were carried out at the B3LYP/6-31G** level for C, N, Se, H, O in the Gaussian 09 program. Cyclic voltammograms were recorded on an electrochemical analyzer (CH Instruments, model no: 600 E Series) using glassy carbon as the working electrode, Pt wire as the counter electrode, and saturated Ag/AgCl as the reference electrode. The scan rate was 100 mV s^{-1} for CV measurements. A solution of tetrabutylammonium hexafluorophosphate ($TBAPF_6$) in DCM (0.1 M) was employed as the supporting electrolyte.

Synthesis. Here, we have synthesized compounds **1**, **2**, and **3** by the Suzuki coupling reaction between 4,7-dibromo-2,1,3-benzoselenadiazole and boronic acid of corresponding donor and acceptor units at different reaction conditions.

Synthesis of 2,1,3-Benzoselenadiazole ***5***. 2,1,3-Benzoselenadiazole **5** was prepared from *o*-phenylenediamine **4** according to a previously reported method[25] and obtained as a faint pink colored solid (54.9 mmol, 98.9%). ^{1}H NMR (400 MHz, $CDCl_3$) δ 7.83 (d, J = 9.5 Hz, 2H), 7.45 (d, J = 9.8 Hz, 2H). ^{13}C NMR (100 MHz, $CDCl_3$) δ 160.50, 129.44, 123.43.

Synthesis of 4,7-Dibromo-2,1,3-benzoselenadiazole ***6***. 4,7-Dibromo-2,1,3-benzoselenadiazole **6** was prepared from **5** according to previously reported method[26] and obtained as golden yellow needles (4.06 mmol, 74.6%). ^{1}H NMR (400 MHz, $CDCl_3$) δ 7.64 (s, 2H). ^{13}C NMR (100 MHz, $CDCl_3$) δ 157.21, 132.14, 116.51.

Synthesis of Compound ***2***. In a 100 mL two neck round-bottom flask, 4,7-dibromo-2,1,3-benzoselenadiazole (300 mg, 0.882 mmol) and naphthalene-1-boronic acid (379 mg, 2.205 mmol) were dissolved in THF (30 mL). Potassium carbonate (1.22 g, 8.82 mmol) was dissolved in 10 mL of water and added to the previous mixture. The reaction mixture was purged with nitrogen gas for 20 min. $Pd(PPh_3)_4$ (55 mg, 0.05 mmol) was added to the reaction mixture. The reaction mixture was stirred overnight at 85 °C. The solvent was removed under reduced pressure. The product was extracted using dichloromethane and washed with Milli-Q water followed by brine solution (3 × 30 mL). The organic part was dried over sodium sulfate, and the solvent was evaporated using rotary evaporator. Purified compound **2** was obtained as a yellow solid powder (0.632 mmol, 72%). ^{1}H NMR (400 MHz, $CDCl_3$) δ 7.96—8.01 (m, 4H), 7.63—7.70 (m, 8H), 7.53 (t, J = 7.4 Hz, 2H), 7.43 (m, 2H); ^{13}C NMR (100 MHz, $CDCl_3$) δ 160.25, 135.94, 135.01, 133.75, 132.01, 130.26, 128.84, 128.51, 127.84, 126.12, 126.01, 125.96, 125.34. HRMS (ESI-TOF) m/z: $(M + Na)^+$ calcd for $C_{26}H_{16}N_2SeNa$ 459.0376, found 459.0372.

Synthesis of Compounds ***1*** *and* ***3***. In a 100 mL two neck round-bottom flask, 4,7-dibromo-2,1,3-benzoselenadiazole (300 mg, 0.882 mmol), potassium carbonate (1.22 g, 8.82 mmol), and para-substituted boronic acid (2.205 mmol) were mixed in water (5 mL) and THF (20 mL). The reaction mixture was purged with nitrogen gas for 20 min. $Pd(PPh_3)_4$ (55 mg, 0.05 mmol) was added to the reaction mixture. The reaction mixture was stirred overnight at 80 °C. The solvent was removed under reduced pressure. The product was extracted using dichloromethane and washed with Milli-Q water followed by brine solution. The organic part was dried over sodium sulfate, and the solvent was evaporated using a rotary evaporator.

Purified compound **1** was obtained as an orange solid powder (0.712 mmol, 81%). ^{1}H NMR (400 MHz, $CDCl_3$) δ 7.83 (d, J = 7.8 Hz, 4H), 7.56 (s, 2H), 7.06 (d, J = 7.8 Hz, 2H), 3.81 (s, 6H). ^{13}C NMR (100 MHz, $CDCl_3$) δ 159.93, 159.65, 134.17, 130.61, 127.81, 113.95, 55.38. HRMS (ESI-TOF) m/z: $(M + Na)^+$ calcd for $C_{20}H_{16}N_2O_2SeNa$ 419.0270, found 419.0279.

Purified compound **3** was obtained as a yellow solid powder (0.58 mmol, 66%). ^{1}H NMR (400 MHz, $CDCl_3$) δ 8.40 (d, J = 8.2 Hz, 4H), 8.10 (d, J = 8.2 Hz, 4H), 7.77 (s, 2H). ^{13}C NMR (100 MHz, $CDCl_3$) δ 143.48, 130.08, 128.76, 123.43. HRMS (ESI-TOF) m/z: $(M + Na)^+$ calcd for $C_{18}H_{10}N_4O_4SeK$ 464.9504, found 464.9504.

Crystal Structure Solution and Refinement. Crystallographic data for compounds **1** and **2** were collected on a Rigaku FRX microfocus rotating anode (3 kW) and a Rigaku MM007 HF (1.2 kW)

DOI: 10.1021/acs.cgd.5b01179
Cryst. Growth Des. XXXX, XXX, XXX—XXX

at the copper Kα edge equipped with a Dectris Pilatus 200 K hybrid detector and R-AXIS SPIDER image plate (IP) respectively. The diffraction intensities were integrated and scaled with the CrystalClear suite version 2.1b25 and 2.1b43. Both structures were solved using SHELXT and refined with SHELXL 2015 version. Full-matrix least-squares refinement were performed on F^2 for all unique reflections, minimizing $w(F_o^2 - F_c^2)^3$, with anisotropic displacement parameters for non-hydrogen atoms. All H atoms found in difference electron-density maps were refined freely, and all the others were treated as riding on their parent C or N atoms. Data statistics are reported in the Table S1 and CIF files.[27]

RESULTS AND DISCUSSION

To elucidate the role of electron donating and accepting units attached with benzoselenadiazole (BDS), we synthesized 4-methoxybenzene (compound **1**), naphthalene (compound **2**), and 4-nitrobenzene (compound **3**) capped benzoselenadiazoles. Syntheses of compounds **1**, **2**, and **3** were achieved by Suzuki coupling reaction shown in Scheme 1. To synthesize these three compounds, first we synthesized benzoselenadiazole with the reaction between *o*-phenylenediamine and selenium dioxide. Four and seven positions of benzoselenadiazole were brominated in the presence of bromine, silver sulfate, and concentrated sulfuric acid. The 4,7-dibromo benzoselenadiazole was treated with corresponding boronic acids in the presence of potassium carbonate and tetrakis triphenylphosphene palladium (0) as a catalyst at 80 °C to synthesize compounds **1**, **2**, and **3** respectively. All three compounds were well characterized by ^{1}H NMR, ^{13}C NMR, and mass spectral studies.

Optical Properties. The absorption and emission spectra of all three compounds in dichloromethane solutions are shown in Figure 2, and all data are summarized in Table 1. The absorption spectra of compounds **1**−**3** possess a characteristic dual-band nature. The higher-energy bands (333−337 nm) are attributed due to the $\pi \rightarrow \pi^*$ transition of the conjugated backbones. The lower-energy bands (390−432 nm) are assigned to charge transfer transitions (CT). The λ_{max} of the higher-energy band remains relatively constant for all three compounds **1**−**3**. The lower-energy charge transfer band is blue-shifted upon moving from compound **1** to compound **3**. Compound **1** shows an internal charge transfer (ICT) band at a significantly higher wavelength as 4-methoxybenzene is a stronger donor unit. The charge transfer band for compound **3** is blue-shifted due to the presence of strong electron withdrawing group.

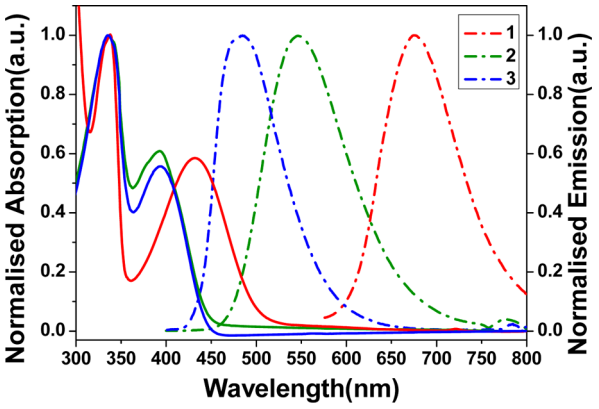

Figure 2. Absorption and emission spectra of compounds **1**−**3** in dichloromethane solutions.

Emission spectra of compounds **1**−**3** were recorded in dichloromethane (DCM) via excitation at the corresponding λ_{max} of lower energy bands. Compounds **1**−**3** exhibit emission maxima at 675, 546, and 483 nm with Stokes shifts of 8334, 7130, and 4937 cm^{-1}, respectively. A small Stokes shift is observed upon attachment of electron withdrawing units (4-nitrobenzene) with benzoselenadiazole (compound **3**) unit. A larger Stokes shift is found when electron donating units are attached with benezoselenadiazole moiety (compound **2**). The most dramatic Stokes shift is observed for compound **1** when stronger donor units (4-methoxybenzene) are attached with an electron accepting unit benzoselenadiazole. The absorption peak at lower energy band is shifted to visible wavelength at 432 nm, and the emission is shifted to 675 nm. The long wavelength emission is attributed to an internal charge transfer (ICT) state.[28]

Electrochemical Properties. The role of electron donating as well as electron withdrawing units on the redox behavior of 2,1,3-benzoselenadiazole based systems **1**−**3** was investigated by cyclic voltammetry studies (Figure S2). Compounds **1**−**3** show the oxidation potentials at 1.23, 1.46, and 1.56 V respectively and the corresponding reduction peaks in the region of −1.005 to −1.108 V. Corresponding band gaps of compounds **1**−**3** were calculated as 2.34, 2.55, and 2.58 eV respectively.[29] The lowest and highest band gaps were observed for compounds **1** and **3** respectively, due to the presence of strong donating and withdrawing groups at the para position of the benzene ring which was capped with 2,1,3-benzoselenadiazole.

Thermogravimetric Analysis. To examine the thermal stability, compounds **1**−**3** were heated at 10 °C min^{-1} under the nitrogen atmosphere (Figure 3). The decomposition temperatures at 5% weight loss of compounds **1**−**3** were calculated as 237, 306, and 184 °C respectively. So the thermal stability of compound **2** is higher up to 5% weight loss of the compound. Again the decomposition temperature at 40% weight loss of compounds **1**−**3** was 344, 371, and 383 °C

Table 1. Photophysical and Electrochemical Properties of Compounds 1−3

	photophysical properties			electrochemical properties			
compound	absorption ($\lambda_{max,abs}$ (nm))	emission ($\lambda_{max,em}$ (nm))	Stokes shift (cm^{-1})	E_{ox} (V)[a]	HOMO (eV)	LUMO (eV)	energy gap (eV)
1	337	675	8334	1.23	−5.69	−3.35	2.34
	432						
2	335	546	7130	1.46	−5.92	−3.37	2.55
	393						
3	333	483	4937	1.56	−6.02	−3.44	2.58
	390						

[a]The values in parentheses corresponds to oxidation potential of small molecules.

DOI: 10.1021/acs.cgd.5b01179
Cryst. Growth Des. XXXX, XXX, XXX−XXX

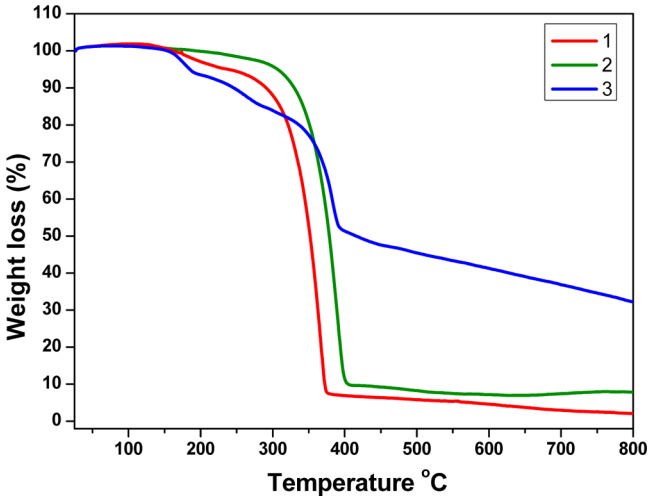

Figure 3. TGA thermograms of compounds **1**–**3** at a heating rate of 10 °C/min under nitrogen gas.

respectively. So, the thermal stability of compound **3** is higher as the decomposition temperature is higher for compound **3** (Table S3).

Molecular Packing of Compounds 1 and 2. Single crystal analysis of molecules is important to understand the packing patterns in the solid state. Single crystals suitable for X-ray diffraction for compounds **1** and **2** were obtained by slow evaporation from dichloromethane at room temperature. Crystallographic data and structure refinement parameters are listed in Table S1. Compounds **1** and **2** were crystallized in the monoclinic $P2_1/n$ and triclinic $P\bar{1}$ space groups, respectively. In crystal structure of compound **1**, two *p*-methoxy phenyl rings are twisted by ∼34° from the central BDS unit, whereas two naphthalene rings are twisted by ∼64° for the crystal structure of compound **2**. Strong Se···N and N···N interactions are observed in compound **2** due to its more twisted nature (Figure 4).

Two molecules are present in the asymmetric unit of the solid state structure of compound **1**. Two molecules form head to head dimers via Se···N interaction with distances of 3.070 and 3.071 Å (Figures 4a and S3). N···N (3.169 Å) interaction is very large which does not participate in crystal packing. Strong Se01···π (3.375 Å) and Se02···π (3.552 Å) interactions are present, which lead to form a twisted structure and interlock type packing along the *a* axis, whereas compound **2** contains only one molecule in the asymmetric unit. It also shows head to head dimerization via Se···N and N···N interactions with intermolecular distances of 2.950 and 2.890 Å, respectively (the van der Waals radii of Se and N is 3.450 Å; and N and N is 3.10 Å) (Figure 4b and S3). Also Se···π (3.434 Å) and CH···π (2.901 Å) inteactions (Figure 4b and S4) are present in the crystal packing of compound **2**. The presence of strong Se···N, N···N, and CH···π interactions lead to interlock-type crystal packing for compound **2**. Two BDS planes in the dimer of compound **1** deviate with a angle of 14.80 Å, whereas the planes of two BDS units in the dimer of compound **2** are almost parallel to each other with Se···N and N···N interactions. The close parallel overlapping of BDS units help to form strong Se···N and N···N interactions in compound **2** compared to compound **1**. D–A–D type benzoselenadiazole-based molecules have a strong tendency to form dimer and interlock-type packing, which also depends on the nature of aromatic rings and the twisted behavior of capped aromatic rings.[22,30] Overall Se···N, π-interaction, D–A interaction, and the nature of capped aromatic rings play an important role in its solid state crystal packing.

Various noncovalent interactions play an important role to form supramolecular assemblies of benzoselenadiazole contain-

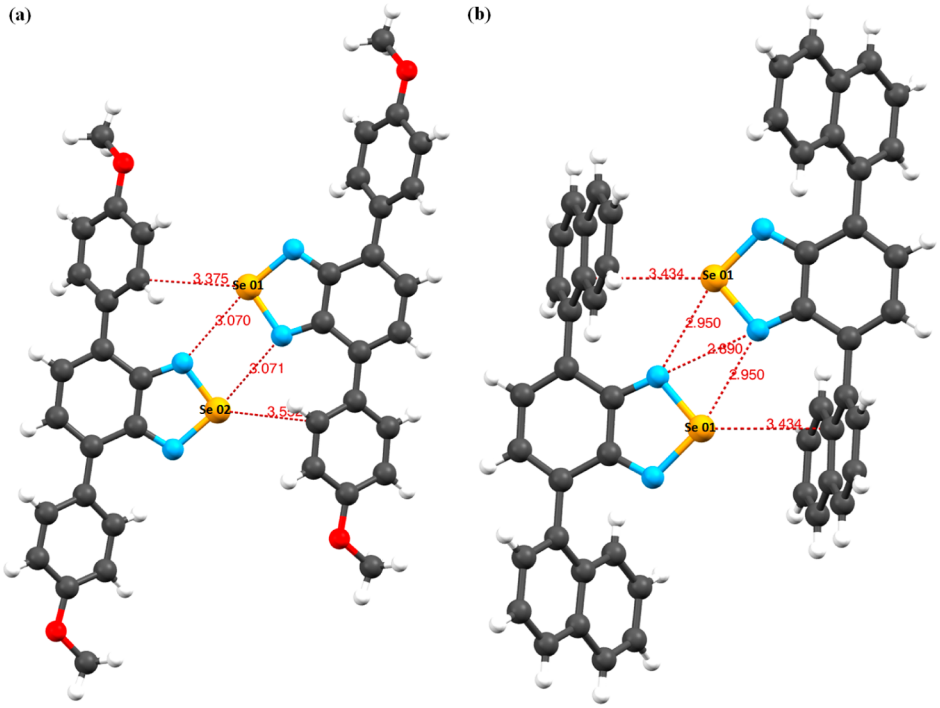

Figure 4. Crystal structure of (a) compound **1** and (b) compound **2**. Intermolecular interactions are responsible for head-to-head dimer formation (interactions are indicated as dotted lines with distance parameters in Å).

DOI: 10.1021/acs.cgd.5b01179
Cryst. Growth Des. XXXX, XXX, XXX–XXX

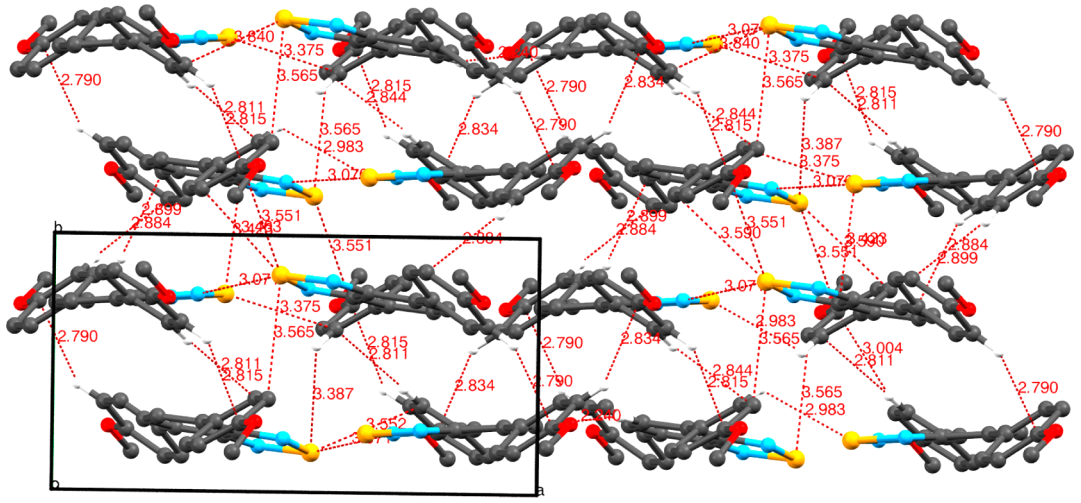

Figure 5. Crystal packing of compound **1** shows various noncovalent interactions (indicated as dotted lines).

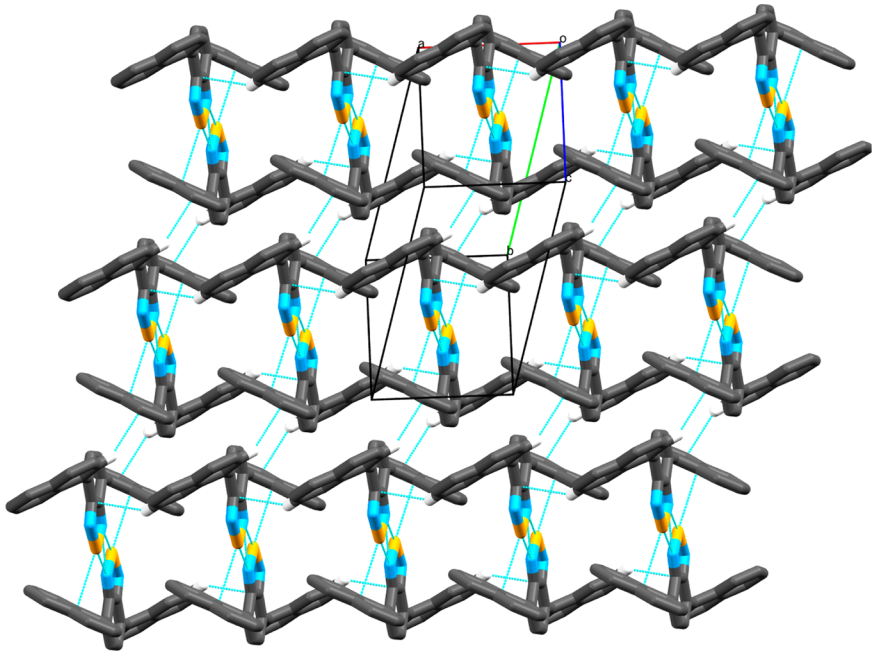

Figure 6. Crystal packing of compound **2** shows a columnar type supramolecular sheet with various noncovalent interactions (indicated as dotted lines). The central dimerized BDS units organized in a face to face manner and hydrophobic naphthyl shoulders are projecting toward columnar rays by interacting with other columnar molecules.

ing compounds which are well characterized by crystallography.[21,22,24,30] In crystal structure, compounds **1** and **2** show well order supramolecular arrangements at the molecular level using noncovalent interactions including Se···π and CH···π interactions (Figures 5 and 6). From the asymmetric unit, it is observed that compound **1** forms dimers to give an interlock-type twisted structure. However, in the process supramolecular assembly in crystal packing, one molecule of the dimer interacts with other neighboring molecules. Se(02) of acceptor benzoselenadiazole and the C(010) atom of donor methoxy phenylene of the neighboring molecule form an Se···π interaction with a distance of 3.463 Å. Additional Se···π interaction is observed in between Se(02) of the acceptor of the neighboring molecule and the C(010) atom of donor methoxy phenylene of the same molecule in the asymmetric unit with a distance of 3.463 Å. Similarly Se01···π (C00S) with a distance of 3.423 Å is observed in between the acceptor benzoselenadiazole and other interacting donor methoxy phenylene residue. Because of strong Se···π interactions between the molecules, other considerable CH···π interactions are also observed between donor methoxy phenylene residues of individual molecules with distances of 2.884 and 2.925 Å (Figures 5 and S5−S6). As a result of these major supramolecular interactions, an interlocked sheet type packing is observed in the crystal structure of compound **1** along the *b* axis.

Similarly compound **2** also forms an interlock-type dimer using strong intermolecular Se···N (2.950 Å), N···N (2.890 Å), Se···π (3.434 Å) and CH···π (2.901 Å) interactions. In the process of a supramolecular arrangement, the dimerized units grow further to form a columnar type of packing pattern by using repeated CH···π (3.132 Å) interactions along the crystallographic *a* axis. There are repeated CH···π (3.132 Å, 2.901 Å) interactions which are observed in between the

DOI: 10.1021/acs.cgd.5b01179
Cryst. Growth Des. XXXX, XXX, XXX−XXX

naphthyl rings of different molecules. As a result of these interactions, a columnar type of supramolecular sheet is formed along the crystallographic *b* axis (Figures 6 and S7).

THEORETICAL STUDY

The density functional theory (DFT) calculations were carried out at the B3LYP/6-31G** level in the Gaussian 09 program. From DFT calculations, we calculated the optimized energy structure, HOMO and LUMO wave functions for all the compounds **1**−**3** (Figure 7). Later, we also calculated the band

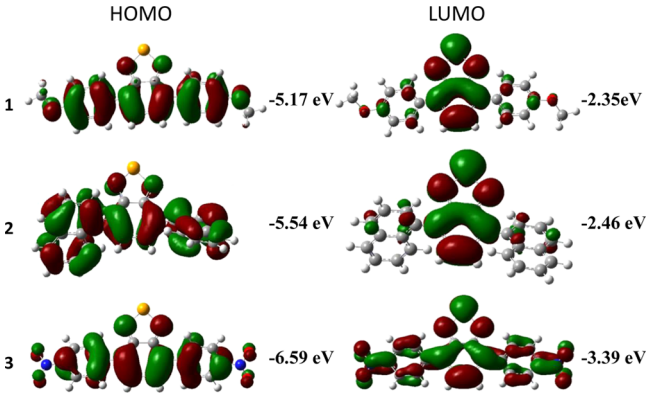

Figure 7. HOMO and LUMO frontier orbitals of compounds **1**−**3** at the B3LYP/6-31G** level for C, N, O, H, and Se.

gap energy of the corresponding molecules. Band gap energy for the compounds **1**−**3** are 2.82, 3.08, and 3.20 eV respectively. HOMO, LUMO, and energy gap of the frontier orbitals of all three compounds are listed in Table S4. The theoretical values show similar trends with the experimental values calculated from cyclic voltametry. The highest and lowest energy gaps for compounds **3** and **1** are exhibited due to the presence of electron withdrawing and donating groups attached with the BDS capped benzene moieties. The LUMO orbitals for compounds **1** and **2** are localized in the central BDS unit, whereas the LUMO orbital in compound **3** is delocalized on the BDS unit to the *p*-nitrobenzene ring.

CONCLUSION

In summary, three conjugated compounds bearing 2,1,3-benzoselenadiazole (BDS) as a centrally located moiety were synthesized by Suzuki coupling reactions between 4,7-dibromo-substituted BDS and corresponding boronic acids. We have investigated the effects of electron donating and accepting units attached with benzoselenadiazole for the change in optoelectronic properties. Electrochemical studies, thermogravimetric analysis, and theoretical studies of 4-methoxybenzene-, naphthalene-, and 4-nitrobenzene-capped benzoselenadiazoles (compounds **1**−**3**) were also performed. Compounds **1**−**3** showed orange, yellow-green, and green colors upon irradiation of UV light at 365 nm. Thermogravimetric analysis showed the highest thermal stability up to a 5% weight loss of naphthalene capped BDS (compound **2**) among three molecules which may be attributed from the higher molecular weight and more closed packing in the crystal structure. Se···N interaction facilitates the formation of head-to-head dimer and also leads to form interlock type packing in the crystal structures of compounds **1** and **2**. Strong intermolecular Se···N, N···N, and C−H···π interactions are observed in the crystal structure of naphthalene capped BDS (compound **2**). The presence of strong Se···N, N···N, and CH···π interactions lead to form interlock type crystal packing. Strong Se01···π (3.375 Å) and Se02···π (3.552 Å, 3.425 Å) interactions present in the crystal structure of compound **1** lead to form a twisted structure and interlock-type packing along the crystallographic *a* axis. Here we tuned the band gap of compounds from 2.34 to 2.58 eV by changing the donor unit 4-methoxybenzene- to acceptor unit 4-nitrobenzene attached with benzoselenadiazole. Theoretical study also supports the change in the band gap by changing the electron donating units to electron withdrawing units attached with benzoselenadiazole.

ASSOCIATED CONTENT

Supporting Information

. The Supporting Information is available free of charge on the ACS Publications website at DOI: 10.1021/acs.cgd.5b01179. The X-ray crystallographic files (CIF) have been deposited in the Cambridge Structural Database with CCDC numbers 1418400 (compound **2**) and 1418401 (compound **1**).

Several experimental results and characterization of compounds **1**−**3** (PDF)

Crystallographic information files (CIF1 and CIF2)

AUTHOR INFORMATION

Corresponding Author

*E-mail: apurba.das@iiti.ac.in.

Notes

The authors declare no competing financial interest.

ACKNOWLEDGMENTS

A.K.D. is thankful to Council of Scientific and Industrial Research (CSIR), New Delhi, India (Grant No. 02(0056)/12/EMR-II) for financial support. M.K. acknowledges CSIR, New Delhi, for his fellowship for this work.

REFERENCES

(1) Li, C.; Liu, M.; Pschirer, N. G.; Baumgarten, M.; Mullen, K. *Chem. Rev.* **2010**, *110*, 6817−6855.
(2) Coughlin, J. E.; Henson, Z. B.; Welch, G. C.; Bazan, G. C. *Acc. Chem. Res.* **2014**, *47*, 257−270.
(3) Yang, J.; Yan, D.; Jones, T. S. *Chem. Rev.* **2015**, *115*, 5570−5603.
(4) Johari, P.; Singh, S. P. *J. Phys. Chem. C* **2015**, *119*, 14890−14899.
(5) Patra, A.; Wijsboom, Y. H.; Zade, S. S.; Li, M.; Sheynin, Y.; Leitus, G.; Bendikov, M. *J. Am. Chem. Soc.* **2008**, *130*, 6734−6735.
(6) Ko, S.; Mondal, R.; Risko, C.; Lee, J. K.; Hong, S.; McGehee, M. D.; Bredas, J. L.; Bao, Z. *Macromolecules* **2010**, *43*, 6685−6698.
(7) Havinga, E. E.; Ten-Hoeve, W.; Wynberg, H. *Polym. Bull.* **1992**, *29*, 119−126.
(8) Caputo, B. J. A.; Welch, G. C.; Kamkar, D. A.; Henson, Z. B.; Nguyen, T.-Q.; Bazan, G. C. *Small* **2011**, *7*, 1422−1426.
(9) Jiang, J.-M.; Yang, P.-A.; Chen, H.-C.; Wei, K.-H. *Chem. Commun.* **2011**, *47*, 8877−8878.
(10) Ozkut, M. I.; Algi, M. P.; Oztas, Z.; Algi, F.; Onal, A. M.; Cihaner, A. *Macromolecules* **2012**, *45*, 729−734.
(11) Pati, P. B.; Das, S.; Zade, S. S. *J. Polym. Sci., Part A: Polym. Chem.* **2012**, *50*, 3996−4003.
(12) Dhanabalan, A.; van Duren, J. K. J.; van Hal, P. A.; van Dongen, J. L. J.; Janssen, R. A. J. *Adv. Funct. Mater.* **2001**, *11*, 255−262.
(13) Horie, M.; Kettle, J.; Yu, C.-Y.; Majewski, L. A.; Chang, S.-W.; Kirkpatrick, J.; Tuladhar, S. M.; Nelson, J.; Saunders, B. R.; Turner, M. L. *J. Mater. Chem.* **2012**, *22*, 381−389.
(14) Distler, A.; Kutka, P.; Sauermann, T.; Egelhaaf, H.-J.; Guldi, D. M.; Di Nuzzo, D.; Meskers, S. C. J.; Janssen, R. A. J. *Chem. Mater.* **2012**, *24*, 4397−4405.

DOI: 10.1021/acs.cgd.5b01179
Cryst. Growth Des. XXXX, XXX, XXX−XXX

(15) Pati, P. B.; Zade, S. S. *Inorg. Chem. Commun.* **2014**, *39*, 114−118.
(16) Cihaner, A.; Algi, F. *Adv. Funct. Mater.* **2008**, *18*, 3583−3589.
(17) Zhou, E.; Cong, J.; Hashimoto, K.; Tajima, K. *Macromolecules* **2013**, *46*, 763−768.
(18) Padhy, H.; Huang, J.-H.; Sahu, D.; Patra, D.; Kekuda, D.; Chu, C.-W.; Lin, H.-C. *J. Polym. Sci., Part A: Polym. Chem.* **2010**, *48*, 4823−4834.
(19) Ekambaram, R.; Enkvist, E.; Manoharan, G.; Ugandi, M.; Kasari, M.; Viht, K.; Knapp, S.; Issinger, O. G.; Uri, A. *Chem. Commun.* **2014**, *50*, 4096−4098.
(20) Saravanan, C.; Easwaramoorthi, S.; Hsiow, C.-Y.; Wang, K.; Hayashi, M.; Wang, L. *Org. Lett.* **2014**, *16*, 354−357.
(21) Ting, H.-C.; Chen, Y.-H.; Lin, L.-Y.; Chou, S.-H.; Liu, Y.-H.; Lin, H.-W.; Wong, K.-T. *ChemSusChem* **2014**, *7*, 457−465.
(22) Pati, P. B.; Zade, S. S. *Cryst. Growth Des.* **2014**, *14*, 1695−1700.
(23) Mikroyannidis, J. A.; Suresh, P.; Sharma, G. D. *Org. Electron.* **2010**, *11*, 311−321.
(24) Dhar, J.; Swathi, K.; Karothu, D. P.; Narayan, K. S.; Patil, S. *ACS Appl. Mater. Interfaces* **2015**, *7*, 670−681.
(25) Gadakh, B.; Vondenhoff, G.; Lescrinier, E.; Rozenski, J.; Froeyen, M.; Van Aerschot, A. *Bioorg. Med. Chem.* **2014**, *22*, 2875−2886.
(26) Yang, R.; Tian, R.; Hou, Q.; Yang, W.; Cao, Y. *Macromolecules* **2003**, *36*, 7453−7460.
(27) Sheldrick. *Acta Crystallogr., Sect. A: Found. Adv.* **2015**, *71*, 3−8.
(28) Diwu, Z.; Lu, Y.; Zhang, C.; Klaubert, D. H.; Haugland, R. P. *Photochem. Photobiol.* **1997**, *66*, 424−431.
(29) Das, S.; Pati, P. B.; Zade, S. S. *Macromolecules* **2012**, *45*, 5410−5417.
(30) Lindner, B. D.; Coombs, B. A.; Schaffroth, M.; Engelhart, J. U.; Tverskoy, O.; Rominger, F.; Hamburger, M.; Bunz, U. H. F. *Org. Lett.* **2013**, *15*, 666−669.

DOI: 10.1021/acs.cgd.5b01179
Cryst. Growth Des. XXXX, XXX, XXX−XXX